Solid Freeform Fabrication 2017: Proceedings of the 28th Annual International Solid Freeform Fabrication Symposium – An Additive Manufacturing Conference
Reviewed Paper

AREAL SURFACE CHARACTERIZATION OF LASER SINTERED PARTS FOR VARIOUS PROCESS PARAMETERS

P. Delfs* and H.-J. Schmid†

* Direct Manufacturing Research Center, Paderborn University, Paderborn, Germany
† Particle Technology Group, Paderborn University, Paderborn, Germany

Abstract

Laser sintered polymer parts consist of rough surfaces due to the layered manufacturing and adherence of incomplete molten particles. The absolute roughness depend on various process parameters like build angle, spatial position, build temperature, exposure order and layer time. Analyses with the help of several areal roughness values of DIN EN ISO 25178-2 considering these parameters are introduced in this paper. Multiple build jobs with 120 µm layer thickness and PA2200 powder were built on an EOS P396 machine using the same build job design with varying process parameters. An individual sample part was designed to receive lots of surface topography information with optical 3D measurements. The results show roughness dependencies for 0° to 180° build angles in 15° steps and eleven distributed in-plane and three axial direction positions depending on different build temperatures, reversed exposure order and layer times. Limitations of the varied parameters are finally derived for the manufacturing of improved surface qualities.

Introduction

It is well known that polymer laser sintered parts possess rough surfaces. Nevertheless, only a few investigation are focused on objective surface roughness values for additive manufactured parts. Mostly, surface roughness is analyzed with the example of the profile arithmetic mean value R_a. Reeves and Cobb [RC97] introduced surface roughness analyses for stereolithography parts with their widespread "truncheon" sample part which covers build angles from 2° to 180° in 2° steps. Later, Upcraft and Fletcher [UF03] demonstrated in their review article advantages and challenges of several additive manufacturing processes including a surface roughness comparison depending on layer thickness and a build angle between 10° to 90°. Bacchewar et al. [BSP07] introduced an ANOVA study and analysis of process parameter influences on surface roughness. They investigated how the parameters build orientation, laser power, layer thickness, beam speed and hatch spacing influence the roughness with the example of the profile arithmetic mean value R_a. Build orientation was found to be the significant parameter affecting surface roughness followed by layer thickness for upward directed surfaces and laser power for downward directed surfaces. Correlating results from the metal technology came from Strano et al. [HSE+13] who analyzed and set up a prediction model for laser melting part surfaces of 316L material. They used as well a surface profilometer and a scanning electron microscope for surface analysis. They found in detail an increasing density of spare particles along step edges as the build angle increases.

Furthermore, only a handful examination are public where areal roughness values are applied to laser sintered parts. Thompson et al. [TSG+17] compared different three-dimensional measurement methods, namely confocal microscopy, coherence scanning interferometry, focus variation microscopy and X-ray computed tomography. They applied measurements to selective laser melted Ti6Al4V part surfaces and analyzed them with various areal texture parameters of ISO 25178-2. Grimm at al. [Gri16][GWW17] used confocal microscopy for an evaluation of the feasibility of three-dimensional surface parameters for quality control in additive manufacturing. Furthermore, they automated the surface analysis via an industrial six-axis robot and applied measurements to laser sintering and laser melting part surfaces.

This work is focused on the application of areal roughness values to laser sintered part surfaces. A systematic approach with high statistic results was aimed at. The presented results of this work contain process parameter variations for a fixed machine type, layer thickness, powder batch and exposure parameters and its influences on surface roughness values.

Basics and measurement conditions

The analyses of all the surfaces were done via defined texture values of DIN EN ISO 25178-2. In detail, the values areal arithmetic mean S_a and areal roughness depth S_z were considered, where S_a is defined as follows:

$$S_a = \frac{1}{A} \iint_A |z(x,y)| \, dx \, dy$$

S_z is defined as the sum of the highest peak and the deepest valley point of the considered area.

The measurements were produced with a "3D-Macroscope VR-3100" of Keyence Corporation. This system operates with fringe light projection as shown in figure 1. A tilted light source projects fringe light pattern onto the sample and a CMOS detector collects the reflected light. Via triangulation, the height information is then derived. A resulting exemplary surface measurement of a 15° tilted surface is also shown in figure 1, where the stair-stepping effect and adhered particles are obvious.

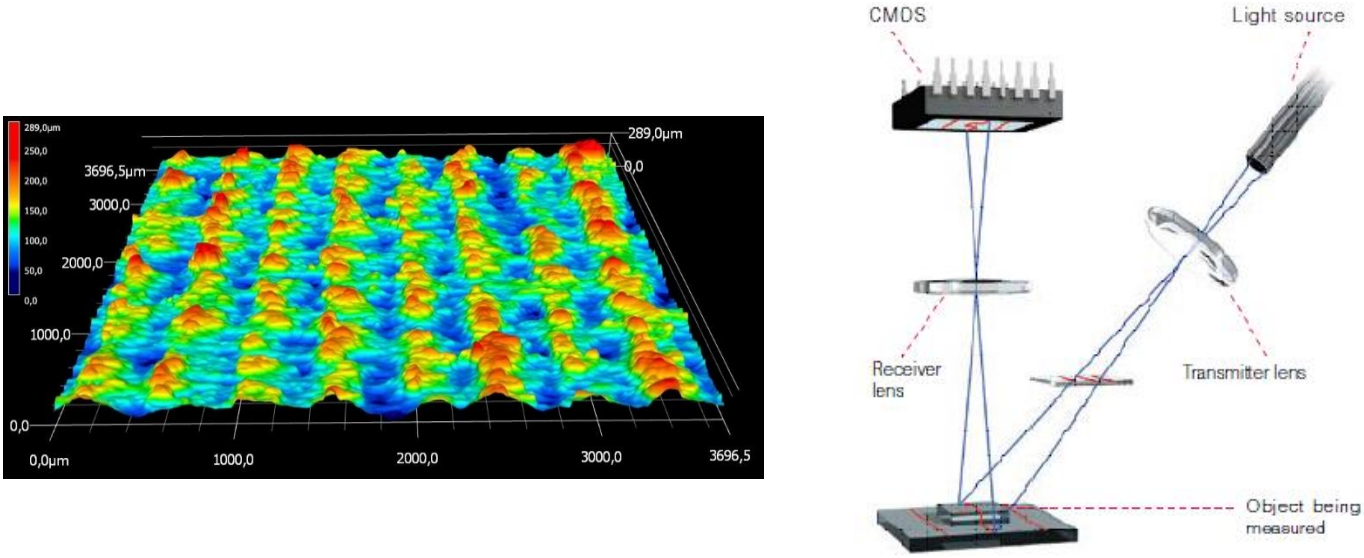

Figure 1: Exemplary 3D-measurement of 15° tilted LS surface (left) and measuring principle of fringe light projection (right).

The measurement area of all measurements are approx. 7 x 9 mm². The corresponding S_a value is calculated by the whole data points. The S_z value is calculated for nine different sub-areas of 2 x 2 mm² size for each measurement to reduce the influence of individual particle agglomerations. The build angle range of 0° to 180° in 15° steps is covered by the hexagon sample part demonstrated in figure 2. The definition of surface angle directions are also given in the two sketches. 0° is a surface parallel to the building platform and upward directed, 90° is a surface orthogonal to the building platform and 180° is a surface downward directed into the powder bed. The angles are shown with front views of the two necessary orientations the sample part has to build with. The basis of the part is formed by a hexagon with feed sizes of 18 mm and 20 mm, which is extruded for 18 mm. The part is hollowed and consists of a wall thickness of 3 mm. Lastly, the center has a 10 mm sized quadratic extruded cut for reproducible post-processing purposes. The design of the sample part enables the part to stand on every surface while the opposing surface is aligned parallel to the ground. This feature allows a constant plane measurement of each surface from the part with the measuring system without the need of a special bracket.

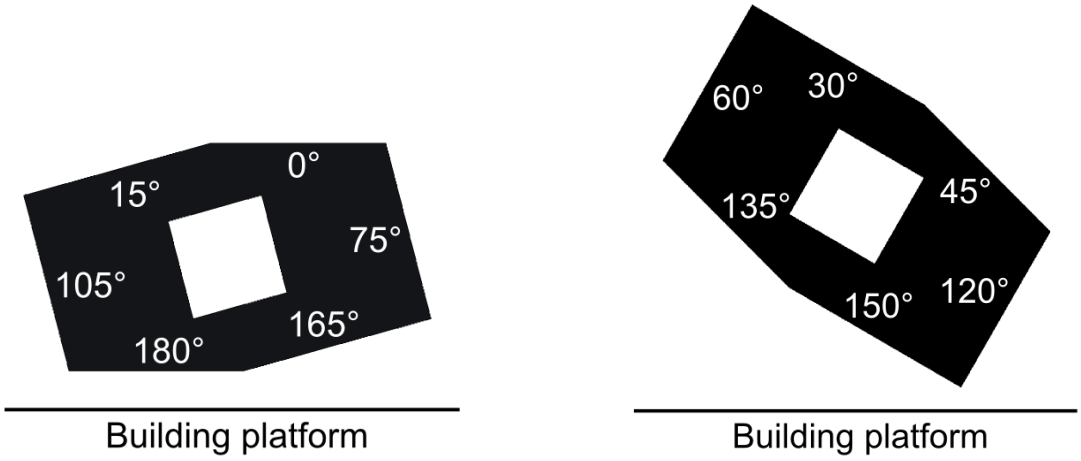

Figure 2: Two build orientations of hexagon sample part with appropriate build angles.

Experimental design

For the manufacturing of sample parts one build job design was prepared, see left image of figure 3. For the analyses covered here, only the blue hexagon parts of the design are of relevance. The whole build space of a EOS P396 machine (350 x 350 x 620 mm³) minus small part free margins on each side is used with sample parts. The hexagon parts are manufactured at three z-height levels, each level with two layers of parts in above-mentioned two orientations. Each layer of parts consists of 22 parts positioned in a 5 x 9 position matrix as shown on the right side in figure 3. The red marked positions are the ones that were measured and analyzed. The dashed lines in red and black indicate center and outside areas. The presented build job was manufactured with various process parameters. Following parameters were held constant for each job:

- Machine: EOS P395
- Material: PA 2200 mixed powder of one batch
- PartPropertyProfile Balance: 120 µm layer thickness
- Preheating time: 4 hours
- Unpacking temperature: below 50 °C

The results of four different build jobs are included here. The variation contains firstly the build temperature, changed by 2 K, and further a reversed exposure order of the parts and an additional 30 s layer time, which is summarized in table 1. A reversed exposure order changes the duration the molten bath is covered with powder material. In build job #4 a dummy part extends this time by 30 seconds, which is approx. four times the exposure duration of the hexagon parts.

Table 1: Overview of build jobs and their varied process parameters.

Build job number	Build temperature / °C	Detailed variation
#1	172.5	-
#2	174.5	-
#3	174.5	reversed exposure order
#4	174.5	plus 30 s layer time

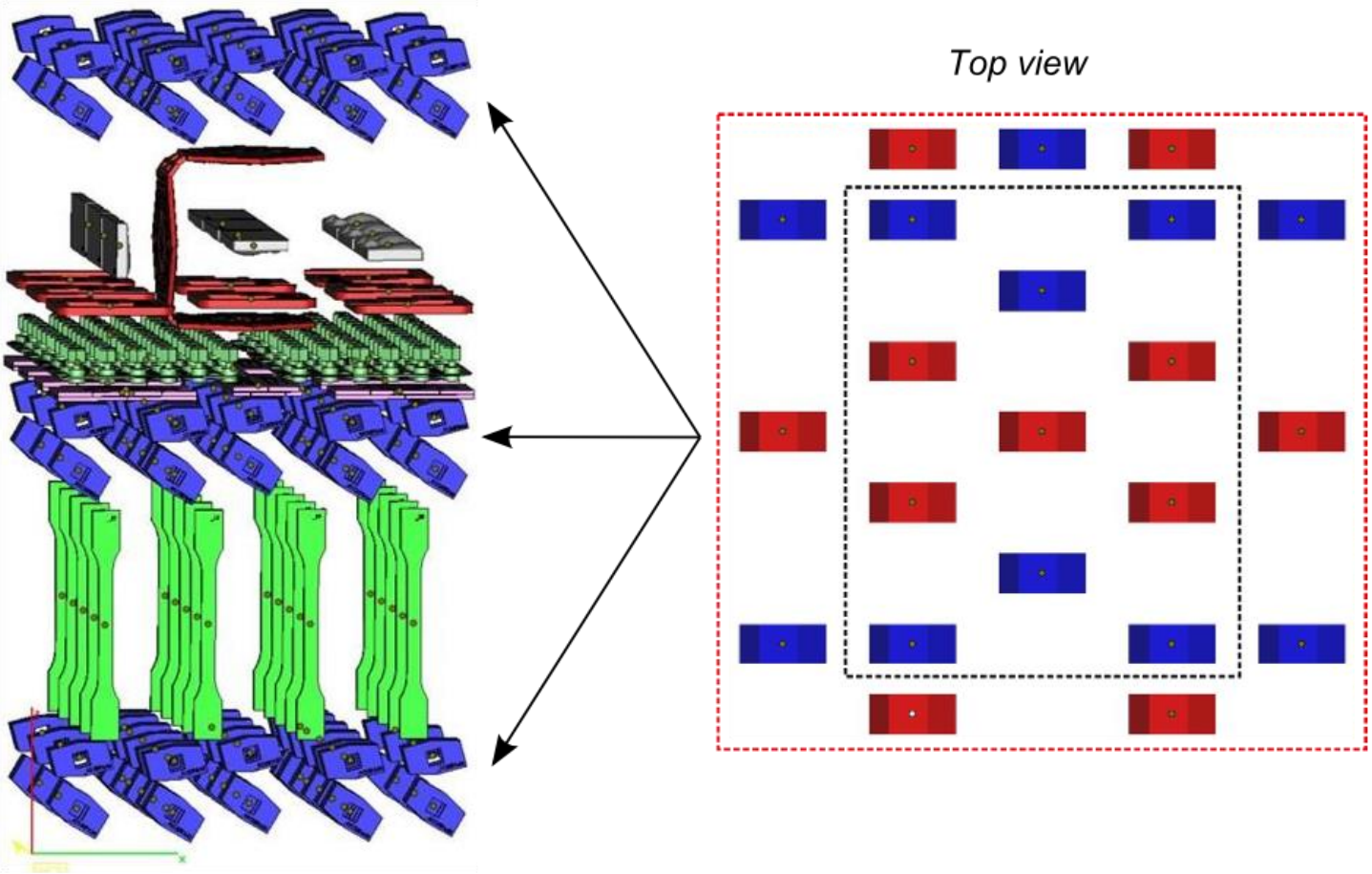

Figure 3: Build job design with top view of x-y-distribution of hexagon samples and division in center (black dashed line) and outside positions (red dashed line).

Results and discussion

The first results show the roughness values S_a and S_z in dependency of the build angle and the four different build jobs in figure 4 and 5. Each data point is the mean value of 33 samples for the distinct build job, averaging all spatial positions. Beginning with the results of S_a values the flat surfaces (0° and 180°) show the lowest values followed by 90° surfaces. Upward directed surfaces (15° to 75°) exhibit a decreasing roughness with increasing angle correlated to a cosine relationship due to the stair-stepping effect of the layer wise manufacturing principle. This effect is strongly diminished for downward directed surfaces (105° to 165°) where all angles appear to be comparable rough. Explanatory approaches are a small curling effect on each layers edge and the filleting effect due to the laser penetration geometry [BSP07]. The standard deviations of the most points are overlapping, nevertheless a light tendency can be seen for build job #4 comprising the lowest the roughness values of all build jobs. The areal roughness depth do not confirm this trend, nearly all values for each build angle are on the same range. Rather noticeable are the even more comparable values for the downward directed surfaces and that they are all lower than the roughness depth of 90° surfaces.

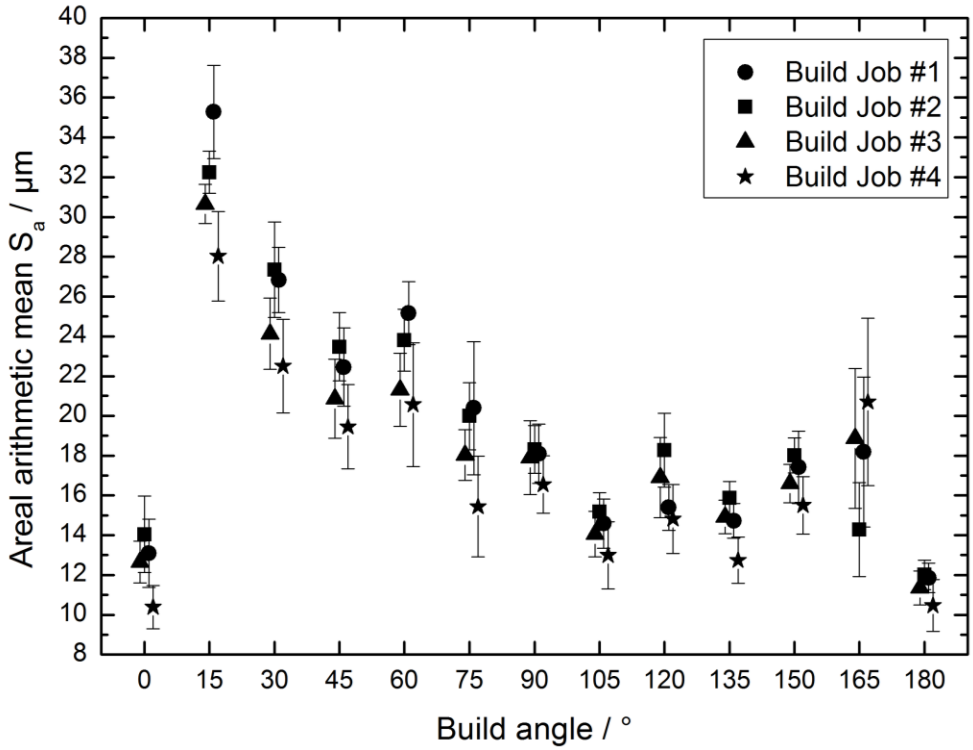

Figure 4: Areal arithmetic mean roughness in dependency of the build angle for all build jobs.

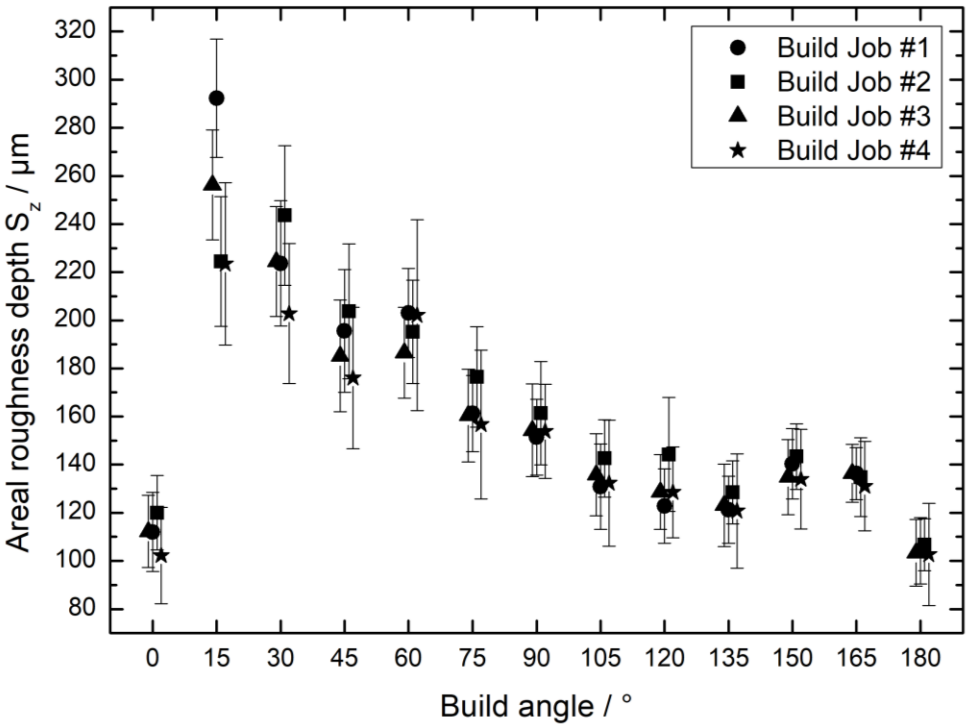

Figure 5: Areal roughness depth in dependency of the build angle for all build jobs.

For a view on spatial dependencies, analyses according the z-height and x-y-distribution are discussed in the following. In figure 6, the z-height dependency is demonstrated exemplarily for build job #3 and the build angles 0°, 15° and 90° as they represent the extreme points in roughness. Per plane the results of eleven samples were averaged, distinct deviations on individual positions were not found. Also, the comparison of different build heights show no differences beyond standard deviations.

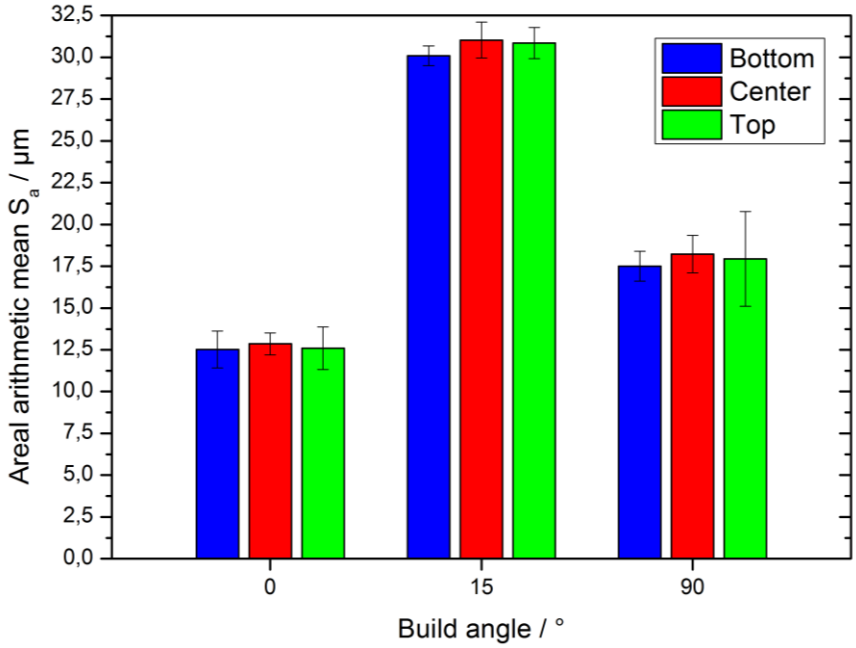

Figure 6: Areal arithmetic mean roughness in dependency of the Z-height for build job #3.

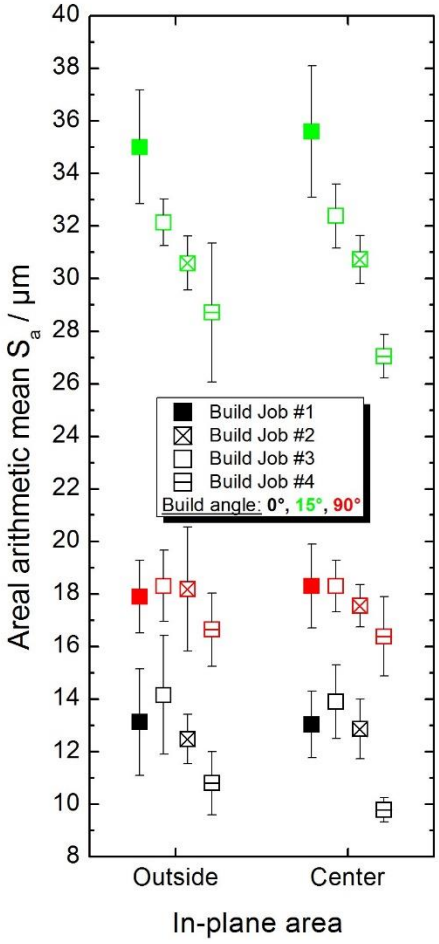

In figure 7, the X-Y-Distribution is shown by separating sample of the center and outside build area as defined in figure 3. Again, the extreme points with 0°, 15° and 90° build angles are selected to exhibit the qualitative tendencies. Measurements of all build heights are averaged as this has no influence like shown before. Distinct differences can hardly be highlighted. Once more, disparities for the in-plane position can not be found while they appear between the different build jobs. Build job #4 possess the smoothest surfaces, which confirms the influence of increased layer time. For 15° build angle also the increased build temperature has a small positive effect on the roughness. The small differences between build job #2 and #3 demonstrate the degree of reproducibility.

Figure 7: Areal arithmetic mean roughness in dependency of the X-Y-Position for all build jobs and 0°, 15° and 90° build angle.

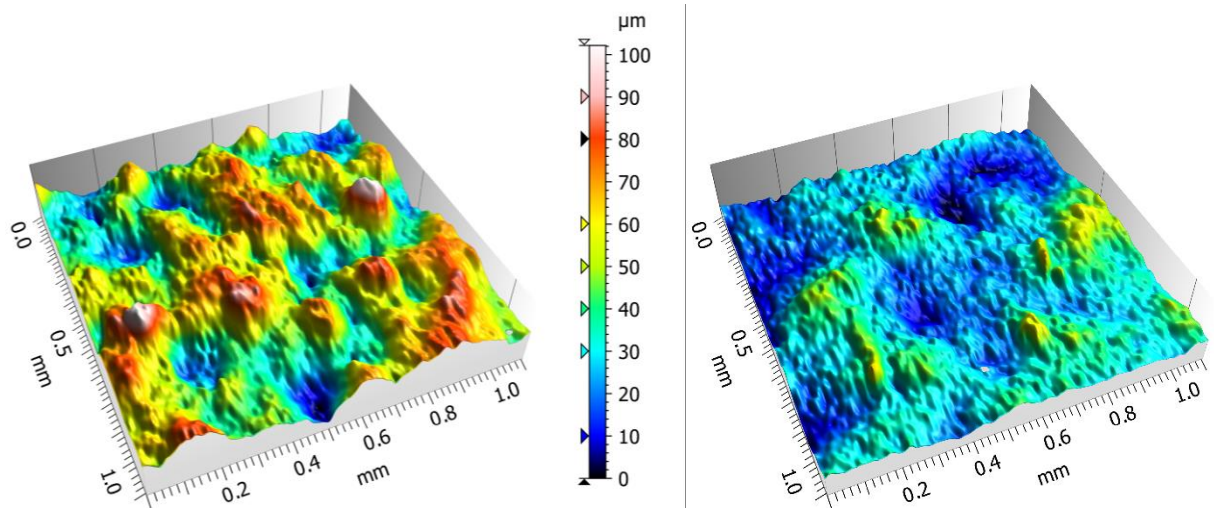

Figure 8: Zoomed 3D-images of 0° surfaces of build job #2 (left) and build job #4 (right) with increased layer time.

An approach for the explanation of smoother surfaces for the build job with increased layer time is demonstrated with exemplary 3D-measurements of 0° build angle surfaces of build job #2 and #4 in figure 8. For this flat surfaces only adhered particles and no stair-stepping effect is responsible for the surface roughness. Both shown images have the same color scale and the differences in local topography gradients are obvious. In the left image the particles protrude much more than in the right image. The increased layer time for the right part surface provides the adhered particles time to melt more into the surface. The adherence of unmolten particles proceed due to the unavoidable contact of the molten bath and particles of the next powder layer. The heat conduction of the material is very low as well as the viscosity just a few degrees over melting temperature. Hence, the degree of particle melt is mostly driven by the available time with IR-heating from above before the next colder layer of powder is deposited and supposed to abort the adherence process. Figure 9 sketches the progress of particle adherence to a molten bath and a time correlation to the layer times of build jobs #2 and #4.

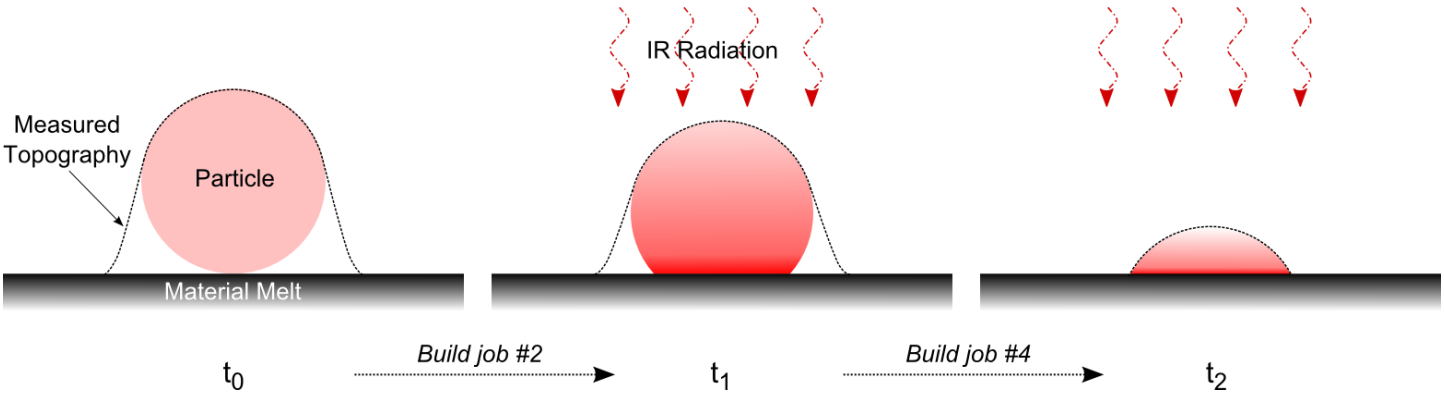

Figure 9: Sketch of particle adherence progress over time after the last laser exposed layer.

Conclusion and outlook

In this paper we demonstrated surface roughness analyses of polymer laser sintered part surfaces via areal surface texture values of DIN EN ISO 25178-2. Build orientation, spatial position, build temperature, exposure order and layer time are varied parameters of the investigations. It was shown that the build orientation has the highest influence on surface roughness followed by the layer where longer durations lead to smoother surfaces. Spatial position, build temperature and exposure order play a minor role.

Further analyses are in preparation for an extended variation of parameters e g. machine type, wall thickness, part distance, layer thickness and powder quality. These results will give an even more detailed view of influence factors for the surface quality in polymer laser sintering.

Acknowledgement

The authors want to thank all industry partners of the DMRC as well as the federal state of North Rhine-Westphalia and the University of Paderborn for the financial and operational support within the project "STEP: Surface Topography Analysis and Enhancement of Laser Sintered Parts".

Literature

[RC97] Reeves, E. R; Cobb, R. C.: "Reducing the surface deviation of stereolithography using in-process techniques". Rapid Prototyping Journal, Vol.3, pp. 20 – 31, 1997.

[UF03] Upcraft, S.; Fletcher, R.: "The rapid prototyping technologies". Assembly Automation, Volume 23, pp. 318 – 330, 2003.

[BSP07] Bacchewar, P. B.; Singhal, S. K.; Pandey, P. M.: "Statistical modelling and optimization of surface roughness in the selective laser sintering process". Proc. IMech E, Part B: J. Engineering Manufacture, Vol. 221, pp. 35 – 52, 2007.

[HSE+13] Strano, G.; Hao, L.; Everson, R. M. et al.: "Surface roughness analysis, modelling and prediction in selective laser melting". Journal of Materials Processing Technology, Vol. 213, pp. 589 – 597, 2013.

[TSG+17] Thompson, A.; Senin, N.; Giusca, C. et al.: "Topography of selectively laser melted surfaces: A comparison of different measurement methods". CIRP Annals – Manufacturing Technology, in press, 2017.

[Gri16] Grimm, T.: "Entwicklung und Validierung einer automatisierten, dreidimensionalen Oberflächenanalyse zur Qualitätskontrolle von additive gefertigten Bauteilen". Shaker Verlag, Phd thesis, 2016.

[GWW17] Grimm, T.; Wiora, G.; Witt, G.: "Quality Control of Laser-Beam-Melted Parts by a Correlation Between Their Mechanical Properties and a Three-Dimensional Surface Analysis". JOM, Vol. 69, pp. 544 – 550, 2017.

[Key15] "One-Shot 3D Measurement". Keyence Corporation, Japan, 2013.